Relationship between amino acid transporter activity and radioactive iodine therapy efficacy in differentiated thyroid cancer

AKIHITO KOTANI[1], YOTA TATARA[2], RIKI SAKAMOTO[1], ANDRZEJ WOJCIK[3], YASUSHI MARIYA[4] and SATORU MONZEN[1,5]

[1]Department of Radiation Science, Hirosaki University Graduate School of Health Sciences, Hirosaki, Aomori 036-8564, Japan; [2]Department of Stress Response Science, Biomedical Research Center, Graduate School of Medicine, Hirosaki University, Hirosaki, Aomori 036-8562, Japan; [3]Centre for Radiation Protection Research, Stockholm University, SE-10691 Stockholm, Sweden; [4]Center for Cancer Treatment and Examination, Aomori Rosai Hospital, Hachinohe, Aomori 031-8551, Japan; [5]Research Center for Biomedical Sciences, Hirosaki University, Hirosaki, Aomori 036-8564, Japan

Received February 12, 2025; Accepted July 31, 2025

DOI: 10.3892/or.2025.8993

Abstract. Thyroid cancer is the most common malignant endocrine tumor. Differentiated thyroid cancer (DTC) accounts for 95% of thyroid cancer cases. The primary treatment for intermediate- and high-risk DTC is total thyroidectomy. Postoperatively, serum thyroglobulin (Tg) and anti-Tg antibody (Tg/Ab) levels are monitored to detect residual, recurrent or metastatic disease. Radioactive iodine (^{131}I) therapy is administered orally when Tg and Tg/Ab levels exceed standard levels. Recombinant human thyroid-stimulating hormone (rhTSH) administration methods that do not require thyroid hormone withdrawal treatment and hospitalization have been recommended. However, serum Tg levels, a biomarker of thyroid tissue ablation, are often disturbed by Tg/Ab interference, which is observed in one-quarter of patients with DTC. The present study aimed to elucidate the molecular mechanisms underlying metabolic changes in patients with DTC treated with ^{131}I, and to identify Tg/Ab-independent biomarker candidates using the TPC-1 cell model. Blood serum samples were collected from patients with DTC before and after administration of ^{131}I, which was performed following stimulation with rhTSH. Intra-individual variations in Tg and Tg/Ab levels were observed in the same patients before and after ^{131}I administration. Serum metabolomic analysis showed elevated levels of branched-chain amino acid (BCAA), including valine, leucine and isoleucine, in all 3 patients, who exhibited favorable clinical outcomes. Although the number of cases was limited, this may suggest a possible association between BCAA levels and treatment response. Additionally, while overall boronophenylalanine uptake decreased in the total cell population after ionizing radiation exposure, the surviving viable TPC-1 cells exhibited relatively increased amino acid uptake, assessed using boronophenylalanine as a leucine analog, which corresponded to the findings presented in the cell-based experiments. Higher expression levels of the CD98 cell surface antigen were observed in irradiated TPC-1 cells compared with non-irradiated controls, which may contribute to increased uptake of BCAAs. However, the mRNA expression levels of L-type amino acid transporter type 1 (*LAT1*), L-type amino acid transporter type 2 and *CD98hc* did not change upon exposure to IR. These results indicated that the increased BCAA uptake in IR-exposed DTC cells was a transient response likely mediated by LAT1/CD98hc at the cell surface, as suggested by flow cytometry analysis, despite no corresponding increase in *LAT1* mRNA expression.

Introduction

Thyroid cancer is the most common malignant endocrine tumor, with an increasing incidence, especially among women (1). Differentiated thyroid cancer (DTC), which includes papillary thyroid cancer (PTC) and follicular subtypes, accounts for 95% of all cases (2). The standard treatment for intermediate- and high-risk DTC is total thyroidectomy, followed by postoperative monitoring of serum thyroglobulin (Tg) and Tg antibody (Tg/Ab) levels to detect residual or recurrent disease (3,4). Oral administration of radioactive iodine (^{131}I) is used when the Tg and Tg/Ab levels exceed standard levels. Conventional radioisotope therapy using ^{131}I increases serum thyroid-stimulating hormone (TSH) levels by thyroid hormone withdrawal (THW), promoting ^{131}I accumulation in the remaining DTC tissues (5). However, because THW-induced hypothyroidism increases the risk of complications, and the number of patients waiting for treatment is increasing, recombinant human TSH (rhTSH), which does not require THW treatment and hospitalization, is recommended (3). However, serum Tg levels are often disturbed by Tg/Ab interference, and

Correspondence to: Professor Satoru Monzen, Department of Radiation Science, Hirosaki University Graduate School of Health Sciences, 66-1 Hon-cho, Hirosaki, Aomori 036-8564, Japan
E-mail: monzens@hirosaki-u.ac.jp

Key words: differentiated thyroid cancer, radioisotope therapy, branched-chain amino acid, L-type amino acid transporter 1

this is observed in one-quarter of all patients with DTC (6-8). Therefore, researchers are exploring metabolic and genetic alterations as complementary biomarkers to Tg to improve the assessment of disease status. However, no reliable standard test has been developed (8-10). Additionally, morphology and functionality can be observed using radiological imaging techniques, such as positron emission tomography/computed tomography. However, the levels or presence of Tg and Tg/Ab cannot be visualized using imaging modalities (11). The lack of association between serum Tg levels and antitumor efficacy in Tg/Ab-positive patients makes it difficult to continue ^{131}I therapy (12) and novel therapeutic biomarkers are needed to address this challenge. Mass spectrometry has been used to explore the possibility of using serum metabolomic analysis to quantify metabolites in biological samples (13). Blood metabolites in patients with DTC are likely to include various diagnostic biomarkers, such as altered levels of amino acids (leucine, valine, lysine and tyrosine), lactate, citrate and lipids, including lysophosphatidylcholine and sphingomyelins, according to previous metabolomic studies (14-17). If Tg/Ab is detected as positive during ^{131}I therapy in combination with rhTSH, the identification of a novel metabolite that can complement Tg will allow treatment optimization. Therefore, the present study aimed to elucidate the molecular mechanisms of metabolomic alterations in patients with DTC treated with ^{131}I and to identify Tg/Ab-independent biomarker candidates using a TPC-1 thyroid cancer cell model. Although the clinical sample size was limited, the present study was designed as a proof-of-concept to provide preliminary evidence supported by experimental validation.

Materials and methods

Analysis of patients with thyroid cancer. The present study was approved by the Committee of Medical Ethics of the Hirosaki University Graduate School of Health Sciences (approval no. 2021-050; Hirosaki, Japan). To protect the rights and privacy of the participants, written informed consent was obtained after providing a detailed verbal explanation, and all collected data were anonymized and handled in accordance with ethical guidelines. The present study included 3 patients (2 female patients and 1 male patient; median age, 58 years; age range, 45-81 years) with DTC who received ^{131}I internal therapy with rhTSH (Thyrogen®; Sanofi S.A.) between April 2022 and December 2024 at Aomori Rosai Hospital (Hachinohe, Japan) (Table I). The inclusion criteria were as follows: Age ≥18 years; histologically confirmed differentiated thyroid carcinoma; completion of total thyroidectomy; planned adjuvant ^{131}I therapy with rhTSH stimulation; and provision of informed consent. The exclusion criteria were: Presence of medullary or anaplastic thyroid carcinoma; uncontrolled severe comorbidities (such as renal failure or severe cardiac disease); prior radioiodine therapy within 12 months; and inability to comply with the study procedures. During treatment, clinical information and blood samples were collected. Routine blood tests, including complete blood counts (red blood cells, white blood cells and platelets) and thyroid-related parameters [TSH, free triiodothyronine (FT3), free thyroxine (FT4), Tg and Tg/Ab], were performed at the clinical laboratory of Aomori Rosai Hospital at three timepoints: Before ^{131}I administration (baseline), on the day of ^{131}I administration (day 0) and 30 days after treatment (day 30), consistent with the measurements shown in Fig. 1.

Serum metabolomic analysis. Peripheral blood was collected from patients with DTC using serum separation tubes (BD Biosciences) at two time points: Before the administration of ^{131}I (day 0) and 30 days after administration (day 30), both under Thyrogen stimulation. To minimize the influence of recent dietary intake, patients were instructed to fast for ≥6 h prior to blood collection. The collected sample tubes were stored in a deep freezer (-80˚C) until analysis. Serum metabolomic analysis was performed using liquid chromatography-mass spectrometry (LC-MS) and flow injection analysis-mass spectrometry (FIA-MS), and the AbsoluteIDQ P180 kit (Biocrates, Inc.) was used to quantify metabolites. The analysis was performed using the method described in our previous study (18). The target metabolites were phenyl isothiocyanate-derivatized and analyzed based on internal standards for quantitation. LC-MS and FIA-MS were performed in positive ion mode using electrospray ionization using a high-performance liquid chromatography system (ExionLC™ AD; SCIEX) combined with a QTRAP 6500+ triple quadruple ion trap hybrid mass spectrometer system (SCIEX) operated with Analyst® 1.6.3 software (SCIEX). LC-MS was used to measure amino acids and biogenic amines, and the multiple reaction monitoring (MRM) conditions are shown in Table SI. The MS measurement conditions were as follows: Curtain gas, 45 psi; collision gas, 6 psi; ion spray voltage, 5,500 V; temperature, 500˚C; ion source gas 1, 40 psi; and ion source gas 2, 50 psi. LC separation was performed on a Zorbax Eclipse XDB-C18 column (3x100 mm; 3.5 μm; Agilent Technologies, Inc.) at 40˚C. The mobile phases consisted of solvent A (water with 0.2% formic acid) and solvent B (acetonitrile with 0.2% formic acid). The flow rate was set at 0.5 ml/min. The gradient program was as follows: 0-0.5 min, 0% B; 0.5-5.5 min, linear increase to 95% B; 5.5-6.5 min, held at 95% B; 6.5-7 min, returned to 0% B and equilibrated for the next injection for 1.5 min. FIA-MS measurements included carnitines and acylcarnitines, hydroxy- and dicarboxyacylcarnitines, sphingomyelins and hydroxysphingomyelins, diacyl phosphatidylcholine, acyl-alkyl phosphatidylcholine, lysophosphatidylcholine, and sugar as targets. The MRM conditions for measuring these metabolites are shown in Table SII. The MS settings were the same as those for LC-MS, except that the temperature was 175˚C. The FIA-MS flow program was as follows: 0-1.6 min, 0.03 ml/min; 1.6-2.4 min, linear increase to 0.2 ml/min; 2.4-2.8 min, held at 0.2 ml/min; and 2.8-3.0 min, returned to 0.03 ml/min. The injection volume was 20 μl. As with LC-MS, FIA-MS quantification was performed using isotopically labeled internal standards provided in the AbsoluteIDQ P180 kit to ensure accuracy and reproducibility. All metabolites were identified and quantified using isotopically labeled internal standards and multiple reaction monitoring as optimized and provided by Biocrates, Inc. Table II shows the measurable metabolites and their abbreviations. Amino acids and biogenic amines were quantified using LC-MS, whereas acylcarnitines, phosphatidylcholines, lysophosphatidylcholines, sphingomyelins and hexose were analyzed by FIA-MS. Among these, Fig. 2 highlights representative metabolites from each category

Table I. Clinical characteristics of the study population.

Patient no.	Sex	Age, years	TNM classification	Thyroid hormone replacement after thyroidectomy	External radiotherapy	^{131}I administration
1	F	81	$T_{4a}N_0M_0$	Liothyronine	50 Gy/25 fr	1.11 GBq
2	F	58	$rT_0N_0M_x$		40 Gy/20 fr +	
3	M	45	$pT_{1a}N_{1a}M_0$		20 Gy/10 fr (boost)	

F, female; fr, fractions; M, male.

Table II. List of target metabolites measured with the AbsoluteIDQ P180 kit.

Metabolite class	Number of analysis targets	Abbreviations of analysis objects
Amino acids and biogenic amines	42	Ala, Arg, Asn, Asp, Cit, Gln, Glu, Gly, His, Ile, Leu, Lys, Met, Orn, Phe, Pro, Ser, Thr, Trp, Tyr, Val,Ac-Orn, ADMA, α-AAA, c4-OH-Pro, carnosine, creatinine, DOPA, dopamine, histamine, kynurenine, Met-SO, nitro-Tyr, PEA, putrescine, SDMA, serotonin, spermidine, spermine, t4-OH-Pro, taurine, total DMA
Carnitines and acylcarnitines	26	C0, C2, C3, C3:1, C4, C4:1, C5, C5:1, C6 (C4:1-DC), C6:1, C8, C9, C10, C10:1, C10:2, C12, C12:1, C14, C14:1, C14:2, C16, C16:1, C16:2, C18, C18:1, C18:2
Hydroxy- and dicarboxyacylcarnitines	14	C3-DC (C4-OH), C3-OH, C5-DC (C6-OH), C5-M-DC, C5-OH (C3-DC-M), C5:1-DC, C7-DC, C12-DC, C14:1-OH, C14:2-OH, C16-OH, C16:1-OH, C16:2-OH, C18:1-OH
Sphingomyeline and hydroxysphingomyelins	15	SM (OH) C14:1, SM (OH) C16:1, SM (OH) C22:1, SM (OH) C22:2, SM (OH) C24:1, SM C16:0, SM C16:1, SM C18:0, SM C18:1, SM C20:2, SM C22:3, SM C24:0, SM C24:1, SM C26:0, SM C26:1
Diacyl phosphatidylcholine	38	PC aa C24:0, PC aa C26:0, PC aa C28:1, PC aa C30:0, PC aa C30:2, PC aa C32:0, PC aa C32:1, PC aa C32:2, PC aa C32:3, PC aa C34:1, PC aa C34:2, PC aa C34:3, PC aa C34:4, PC aa C36:0, PC aa C36:1, PC aa C36:2, PC aa C36:3, PC aa C36:4, PC aa C36:5, PC aa C36:6, PC aa C38:0, PC aa C38:1, PC aa C38:3, PC aa C38:4, PC aa C38:5, PC aa C38:6, PC aa C40:1, PC aa C40:2, PC aa C40:3, PC aa C40:4, PC aa C40:5, PC aa C40:6, PC aa C42:0, PC aa C42:1, PC aa C42:2, PC aa C42:4, PC aa C42:5, PC aa C42:6
Acyl-alkyl phosphatidylcholine	38	PC ae C30:0, PC ae C30:1, PC ae C30:2, PC ae C32:1, PC ae C32:2, PC ae C34:0, PC ae C34:1, PC ae C34:2, PC ae C34:3, PC ae C36:0, PC ae C36:1, PC ae C36:2, PC ae C36:3, PC ae C36:4, PC ae C36:5, PC ae C38:0, PC ae C38:1, PC ae C38:2, PC ae C38:3, PC ae C38:4, PC ae C38:5, PC ae C38:6, PC ae C40:1, PC ae C40:2, PC ae C40:3, PC ae C40:4, PC ae C40:5, PC ae C40:6, PC ae C42:0, PC ae C42:1, PC ae C42:2, PC ae C42:3, PC ae C42:4, PC ae C42:5, PC ae C44:3, PC ae C44:4, PC ae C44:5, PC ae C44:6
Lysophosphatidylcholine	14	lysoPC a C14:0, lysoPC a C16:0, lysoPC a C16:1, lysoPC a C17:0, lysoPC a C18:0, lysoPC a C18:1, lysoPC a C18:2, lysoPC a C20:3, lysoPC a C20:4, lysoPC a C24:0, lysoPC a C26:0, lysoPC a C26:1, lysoPC a C28:0, lysoPC a C28:1
Sugar	1	H1
Total	188	-

that showed statistically significant or consistent changes before and after ^{131}I administration. The metabolomics datasets of LC-MS and FIA-MS generated in the present study have been deposited in MetaboBank (https://www.ddbj.nig.ac.jp/metabobank/index-e.html) under the accession numbers MTBKS257 and MTBKS258, respectively. For pathway

enrichment analysis, metabolites that showed significant changes before and after ^{131}I administration were analyzed using MetaboAnalyst 6.0 (https://www.metaboanalyst.ca/) with pathway annotation based on the Kyoto Encyclopedia of Genes and Genomes (KEGG) database (https://www.genome.jp/kegg/).

Cell culture for thyroid cancer cell model. The TPC-1 human thyroid papillary carcinoma cell line was obtained from Merck KGaA. The cells were cultured in RPMI-1640 (Nacalai Tesque, Inc.) containing 10% heat-inactivated fetal bovine serum (Biowest), 2 mM L-glutamine (MilliporeSigma) and 1% penicillin/streptomycin in a humidified atmosphere at 37˚C with 5% CO_2.

Exposure to ionizing radiation (IR) for the basic experiment. TPC-1 cells were irradiated using an X-ray generator (MBR-1520R-3; Hitachi Power Solutions Co., Ltd.) at 1 Gy/min (150 kVp; 20 mA) with 0.5-mm aluminum and 0.3-mm copper filters. The radiation dose was monitored using a thimble ionization chamber. Handling of ^{131}I *in vitro* requires specialized radiation safety measures and licensing, which can impede exploratory studies. Therefore, X-rays were chosen as a practical and controllable radiation source to model general cellular responses to IR independently of sodium/iodide symporter (NIS)-mediated uptake. Based on clonogenic survival assays, an 8 Gy dose was selected for irradiation to ensure ~1% survival of TPC-1 cells. This dose was chosen to induce measurable biological effects relevant to therapeutic radiation exposure while maintaining sufficient cell viability for downstream analyses. Although clinical radioiodine therapy doses vary depending on remnant size and uptake, the 8 Gy dose provides a reproducible and biologically meaningful model to study cellular radiation responses. Clinical absorbed doses to thyroid remnants and metastases are typically much higher (commonly cited targets, ~300 Gy for remnants and ~80 Gy for metastases) (19,20). Cell viability was assessed using a trypan blue exclusion assay. Briefly, 20 μl cell suspension was mixed with 20 μl trypan blue solution (0.4%; 2-fold dilution; Nacalai Tesque, Inc.) at room temperature. The cells were gently mixed and incubated for <3 min to allow dye penetration into nonviable cells. The viable (unstained) and nonviable (blue-stained) cells were then counted using a Bürker-Türk hemocytometer (Erma, Inc.) under a light microscope (IX71; Olympus Corporation) without fixation.

Clonogenic potency assay for TPC-1 cells. Colony-forming cells were counted using a clonogenic potency assay. The cells were plated at a density of 500-8,000 cells/dish in a 35-mm diameter culture dish, irradiated with 0 to 8 Gy of IR and incubated for 6-9 days in a humidified atmosphere at 37˚C with 5% CO_2. The irradiation was delivered at a dose rate of 1 Gy/min, and the exposure time was adjusted according to the prescribed dose. Subsequently, the dishes were fixed with -20˚C cold methanol for 15 min and stained with Giemsa solution (Muto Pure Chemicals Co., Ltd.) at room temperature for 30 min. Colonies containing >50 cells were manually counted under an inverted microscope (IX71; Olympus Corporation). The cell survival rate was calculated relative to the nonirradiated controls and plating efficiency, as described previously (21).

Cell cycle distribution analysis. The cell cycle distribution was analyzed using flow cytometry. The harvested cells were treated with precooled (-20˚C) 70% ethanol for 10 min on ice and stored at -20˚C until measured. RNase I was added to the sample tube at 37˚C for 20 min (5 μg/ml; Merck KGaA) to remove internal RNAs. The cells were then stained with PI (40 μg/ml; FUJIFILM Wako Pure Chemical Corporation) in the dark at room temperature for 2 min. Cell cycle distribution analysis was performed using Cell Lab Quanta™ Sc MPL (Beckman Coulter, Inc.) and analyzed with Kaluza software (version 2.1; Beckman Coulter, Inc.).

Amino acid uptake assay. Amino acid uptake into cells was analyzed using a boronophenylalanine (BPA) uptake assay kit (cat. no. 342-09893; Dojindo Laboratories, Inc.). BPA is an amino acid analog. The cells exposed to IR were plated in a 96-well microplate and incubated for 12 h at 37˚C in a 5% CO_2 incubator. Reagents were added according to the manufacturer's instructions. The fluorescence of the samples (Ex_{350}/Em_{455}) was first measured using a microplate reader (TriStar LB 941; Berthold Technologies GmbH & Co. KG). After this, the incubated cells were harvested and analyzed by flow cytometry (Aria SORP; BD Biosciences) using FACS Diva™ software (ver.6.0; BD Biosciences) to assess BPA uptake at the single-cell level. This assay utilizes a cell-permeable fluorescent probe that binds to intracellular amino acid analogs. Upon uptake of BPA via amino acid transporters such as solute carrier family 7 member 5 [L-type amino acid transporter type 1 (LAT1)], the probe emits fluorescence (λ_{ex}, 360 nm; λ_{em}, 460 nm), allowing quantification of transporter activity in viable individual cells.

CD98 cell surface antigen expression. The expression levels of the CD98 cell surface antigen were analyzed using double staining with PI and CD98-FITC. The harvested cells were suspended in Hanks' balanced salt solution at 4˚C. CD98-FITC (5 μl per 1x10^6 cells in 100 μl staining volume; cat. no. 315603; BioLegend, Inc.) was added to the sample tubes and these were incubated for 20 min on ice (~0˚C) in the dark. After washing with Hanks' balanced salt solution, the samples were stained with PI (40 μg/ml; FUJIFILM Wako Pure Chemical Corporation) for 3 min at room temperature. Cellular fluorescence was measured using Cell Lab Quanta™ Sc MPL (Beckman Coulter, Inc.) and analyzed with Kaluza software (version 2.1; Beckman Coulter, Inc.).

Total RNA extraction and reverse transcription-quantitative PCR (RT-qPCR). Total RNA was extracted from the cells using the RNeasy® Plus Mini Kit (Qiagen, Inc.). The concentration and quality were confirmed using the NanoDrop system (Thermo Fisher Scientific, Inc.). cDNAs were synthesized to analyze mRNA expression using ReverTra Ace qPCR RT Master Mix (Toyobo Co., Ltd.) according to the manufacturer's instructions. The primer sequences for *LAT1*, solute carrier family 7 member 8 [L-type amino acid transporter type 2 (*LAT2*)] and solute carrier family 3 member 2 (*CD98hc*) were designed based on the gene sequences obtained from

Table III. Sequences of human *LAT1*, *LAT2*, *CD98hc* and *B2M* primers used for reverse transcription-quantitative PCR.

Name	Sequence (5'-3')
LAT1-Forward	TACTTCACCACCCTGTCCAC
LAT1-Reverse	TGGAGGATGTGAACAGGGAC
LAT2-Forward	ATTGAGCTGCTAACCCTGGT
LAT2-Reverse	AGGAGAGAGTAGCCAGGGAA
CD98hc-Forward	TCTTGATTGCGGGGACTAAC
CD98hc-Reverse	GCCTTGCCTGAGACAAACTC
B2M-Forward	TTTCATCCATCCGACATTGA
B2M-Reverse	CCTCCATGATGCTGCTTACA

LAT1, L-type amino acid transporter type 1; *LAT2*, L-type amino acid transporter type 2; *CD98hc*, solute carrier family 3 member 2; *B2M*, β-2-microglobulin.

the National Center for Biotechnology Information database (https://www.ncbi.nlm.nih.gov/gene/). The mRNA expression levels were evaluated using RT-qPCR with the Power SYBR™ Green PCR Master Mix (Thermo Fisher Scientific, Inc.) and SmartCycler® II (Takara Bio, Inc.). The thermocycling conditions were: 95˚C for 10 min, followed by 40 cycles of 95˚C for 15 sec and 60˚C for 1 min. The relative expression of each target mRNA was determined using the $2^{-\Delta\Delta Cq}$ method (22). The accession numbers were as follows: *LAT1*, NM_003486.7; *LAT2*, NM_001267036.1; *CD98hc*, NM_001012662.3; and β-2-microglobulin (*B2M*), NM_004048.4. The oligonucleotide primer sets used for RT-qPCR were designed using Primer3 software (version 4.1.0) (23) and supplied by Eurofins Genomics (Table III). *B2M* was selected as the housekeeping gene for normalization based on the Minimum Information for Publication of Quantitative Real-Time PCR Experiments guidelines (24).

Statistical analysis. Statistical analysis was performed using R software (version 4.4.0; https://www.r-project.org/). Cell cycle analysis was conducted using Kaluza software (version 2.1; Beckman Coulter, Inc.) to identify sub-G_1, G_0/G_1, S and G_2/M phases. The clonogenic survival fraction (F) was fitted to the equation $F(D)=\exp(-\alpha D-\beta D^2)$, where D is the dose in Gy and α and β are fitting coefficients, using the Levenberg-Marquardt algorithm. For small sample sizes (n=3), the Wilcoxon signed-rank test was used for paired comparisons involving two timepoints (such as metabolomic data before vs. after ^{131}I administration). For TSH levels measured at three timepoints (before rhTSH, day 0 and day 30), the Friedman test was applied to account for repeated measures across multiple timepoints. This test was chosen as a non-parametric alternative to repeated-measures ANOVA suitable for small sample sizes and non-normal distributions. For comparisons between two independent groups with normal distribution and equal variance, an unpaired Student's t-test was used. For data with unequal variance, Welch's t-test was applied. For comparisons among multiple groups with normal distribution and equal variance, one-way ANOVA was used, followed by the Tukey-Kramer post hoc test for pairwise comparisons. For comparisons of mRNA expression levels among multiple radiation dose groups, one-way ANOVA followed by the Tukey-Kramer post hoc test was used. Data are presented as the mean ± SD. The number of independent experiments ranged between 3 to 10. $P<0.05$ or false discovery rate (FDR) <0.05 was considered to indicate a statistically significant difference.

Results

Patient characteristics during ^{131}I therapy. Of the 3 patients with DTC included in the present study, 2 were female and 1 was male. The patients were diagnosed with PTC (Table I). Additionally, the patients had no previous medical history of other thyroid diseases. Thyrogen was administered twice, 2 days and 1 day before ^{131}I administration, and its accumulation in the residual tumor was observed using scintillation scanning during treatment. Antitumor effects were observed in all patients 6 months after the initial prescription of Thyrogen, as evaluated based on the medical records of the patients (data not shown). No significant hemocytopenia was observed in terms of the numbers of red blood cells, white blood cells and platelets within 30 days after ^{131}I therapy (Fig. 1A-C). Serum TSH levels increased in all patients, reaching a maximum of 105-455 μIU/ml, from before Thyrogen administration to just prior to ^{131}I administration. By day 30 after administration, TSH levels had returned to the same range as before ^{131}I administration (Fig. 1D). FT3 and FT4 before and after treatment remained at 2.6-3.6 pg/ml and 1.4-2.4x10^{-2} ng/ml, respectively, which were confirmed to be normal values (Fig. 1E and F). Conversely, the levels of Tg/Ab and Tg in the serum showed individual variations between patients (patient 1: Tg/Ab, 10-10.6 IU/ml; Tg, 2.24 ng/ml; patient 2: Tg/Ab, 12.6-12.9 IU/ml; Tg, 23.5-35.1 ng/ml; patient 3: Tg/Ab, 10 IU/ml; Tg, 0.07-0.39 ng/ml; Fig. 1G and H).

Patient metabolomic analysis. Metabolomic analysis was performed using patient serum to explore serum metabolites specifically altered by ^{131}I radiotherapy following Thyrogen stimulation for DTC. Of the 188 types of target metabolomic analysis data obtained from mass spectrometry, 168 were highly reliable. Among them, the levels of nine metabolites that changed before and after ^{131}I administration were increased, and the levels of one metabolite were decreased (Fig. 2). Furthermore, enrichment analysis based on the KEGG database using MeatboAnalyst6.0 identified valine, leucine and isoleucine biosynthesis as a significant metabolic pathway (FDR, 0.0392; data not shown). Valine, leucine and isoleucine are essential amino acids referred to as branched-chain amino acids (BCAAs) and are involved in the nitrogen supply to cancer (25). In all cases, BCAA levels tended to increase after ^{131}I administration compared with before administration (Fig. 2). However, statistical significance was observed only for valine, whereas the increases in leucine and isoleucine were not significant. Given the small sample size (n=3), statistical comparisons were performed using the Wilcoxon signed-rank test. The consistent upward trend across patients supports the robustness of this exploratory observation.

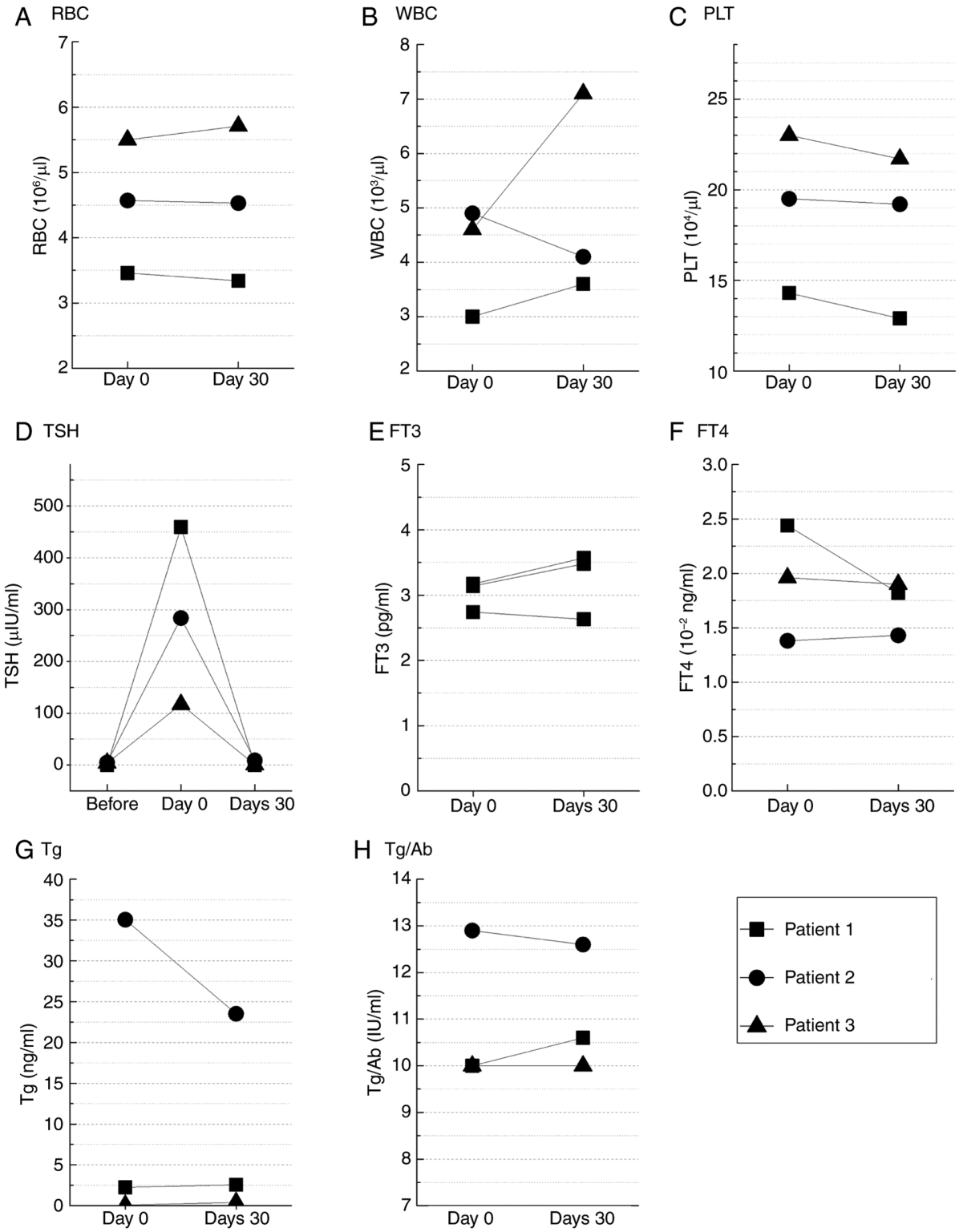

Figure 1. Blood biomarkers measured before ^{131}I administration (baseline), on the day of ^{131}I administration (day 0) and 30 days after treatment (day 30) in 3 patients with differentiated thyroid cancer after thyroidectomy. (A) RBC, (B) WBC, (C) PLT, (D) TSH, (E) FT3, (F) FT4, (G) Tg and (H) Tg/Ab. Statistical analysis was performed using the Wilcoxon signed-rank test for paired comparisons involving two timepoints. For TSH, comparisons across three timepoints were performed using the Friedman test. No significant differences were observed in any of the biomarkers. Normal reference ranges: RBC, 4.0-5.5x10^6/μl; WBC, 4.0-9.0x10^3/μl; PLT, 15-35x10^4/μl; TSH, 0.4-4.0 μIU/ml; FT3, 2.3-4.1 pg/ml; FT4, 0.9-1.7x10^{-2} ng/ml; Tg, <30 ng/ml; Tg/Ab, <40 IU/ml. FT3, free triiodothyronine; FT4, free thyroxine; PLT, platelets; RBC, red blood cells; Tg, thyroglobulin; Tg/Ab, thyroglobulin antibody; TSH, thyroid-stimulating hormone; WBC, white blood cells.

Radiosensitivity of TPC-1 cells. The TPC-1 cell line was used to examine whether the serum metabolic changes observed in patients with DTC could be recapitulated at the cellular level. Clonogenic potency and the cell cycle were analyzed to confirm the radiosensitivity of TPC-1 cells. The plating efficiency for TPC-1 cell colony formation was 13±1.2%

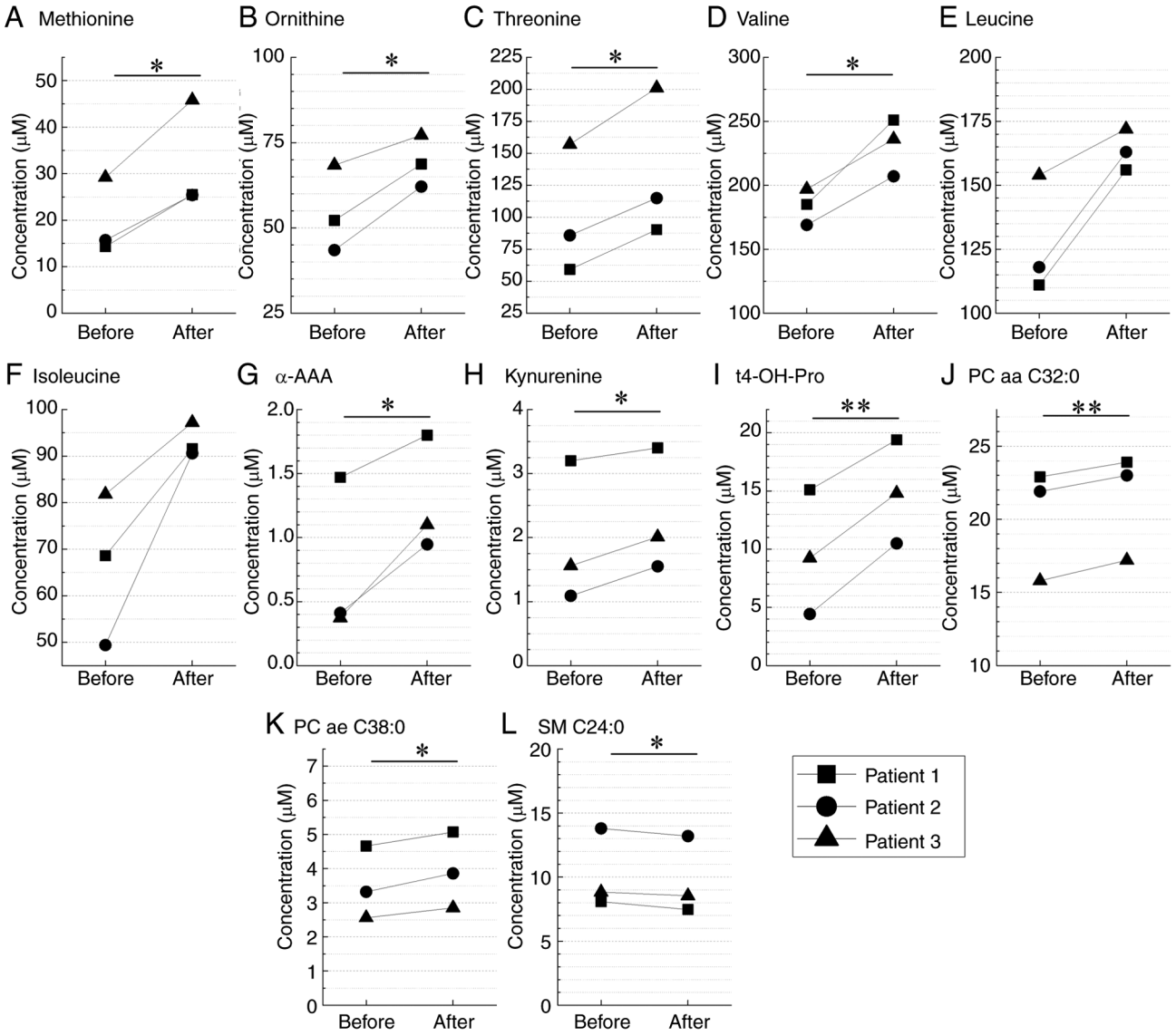

Figure 2. Quantification of serum metabolites using mass spectrometry. Analysis of the serum samples collected from patients with differentiated thyroid cancer before (day 0) and after ^{131}I administration (day 30). The levels of 12 metabolites, namely (A) methionine, (B) ornitine, (C) threonine, (D) valine, (E) leucine, (F) isoleucine, (G) α-AAA, (H) kynurenine, (I) t4-OH-Pro, (J) PC aa C32:0, (K) PC ae C38:0 and (L) SM C24:0, are shown. *P<0.05 and **P<0.01 (Wilcoxon signed-rank test). α-AAA, α-aminoadipic acid; PC aa C32:0, phosphatidylcholine type aa C32:0; PC ae C38:0, phosphatidylcholine type ae C38:0; SM C24:0, sphingomyelin type C24:0; t4-OH-Pro, trans-4-hydroxyprolin.

(Fig. 3A), the parameters in the linear-quadratic model were α=0.32±0.05 Gy^{-1}, β=0.03±0.02 Gy^{-2} and α/β=12.12±0.66, and the survival rate was <1% at 8 Gy (Fig. 3B). The cell cycle phase distribution analysis of cells exposed to 8 Gy IR showed a time-dependent increase in cells in the G_2/M phase for 12 h. A significant increase was observed at 6-24 h compared with the non-irradiated control (Fig. 3C and D). The number of viable cells after 12 h of exposure decreased to ~50% compared with that of the non-irradiated group (Fig. 3E).

Quantitation of BCAA uptake under IR exposure. Similar to BCAAs, BPA is taken up by cells via LAT1 (26,27). Changes in BPA uptake were evaluated to determine the BCAA uptake ability of irradiated TPC-1 cells. After 12 h of exposure to 8 Gy IR, intracellular BPA levels significantly decreased to ~80% of those in the non-irradiated control group, corresponding to an ~20% reduction (Fig. 4A). Conversely, single-cell analysis by flow cytometry revealed that the levels of intracellular BPA following exposure to IR were significantly upregulated ~1.58 times compared with the non-irradiated control (Fig. 4B and C).

CD98 expression. LAT1 forms a complex with CD98hc on the cell membrane and triggers amino acid uptake (28). The flow cytometry analysis of TPC-1 cells exposed to 8 Gy IR revealed significant upregulation of the CD98 cell surface antigen compared with the non-irradiated control (Fig. 5). However, RT-qPCR analysis revealed that the expression levels of the related mRNAs *LAT1*, *LAT2* and *CD98hc* were similar to those in the non-irradiated control group (Fig. 6).

Discussion

In the present study, serum metabolomic analysis focusing on patients with DTC and single-cell analysis using TPC-1 cells

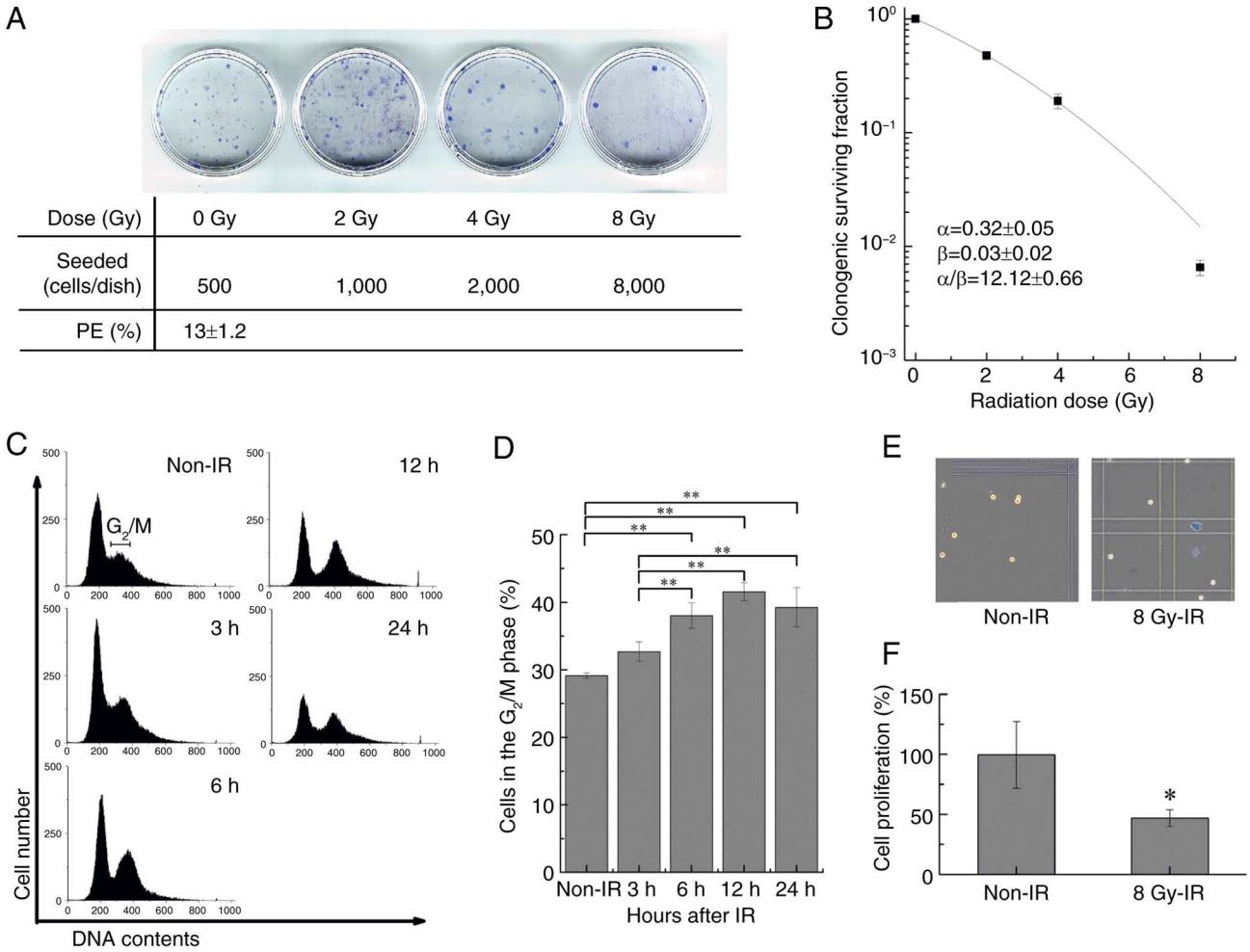

Dose (Gy)	0 Gy	2 Gy	4 Gy	8 Gy
Seeded (cells/dish)	500	1,000	2,000	8,000
PE (%)	13±1.2			

Figure 3. Analysis of radiation responses in TPC-1 cells. (A) Representative images of colony formation after IR exposure in 35-mm dishes. Cells were stained with Giemsa. The corresponding plating efficiency is shown. (B) Clonogenic survival curve showing the surviving fraction of cells exposed to IR ≤8 Gy. (C) Representative histograms of cell cycle distribution. (D) Quantitation of cells in the G_2/M phase. (E) Representative images of trypan blue exclusion assay. The grid shown corresponds to 0.2-mm squares. (F) Percentage of viable cells after 12 h of 8 Gy-IR exposure Data are presented as the mean ± SD of four or five independent experiments. *P<0.05 (Welch two-sample t-test). **P<0.01 (one-way ANOVA with Tukey-Kramer post hoc test). IR, ionizing radiation; PE, plating efficiency.

were conducted to identify Tg/Ab-independent biomarkers that indicate the effect of thyroid cancer ablation using ^{131}I administration under Thyrogen therapy. On day 30 post-treatment, only 1 case showed a response based on Tg levels; however, an increase in BCAA levels, particularly valine, was observed independently of Tg/Ab fluctuations. In the DTC cell model, exposure to 8 Gy IR altered BPA uptake, a leucine analog used to evaluate BCAA transport, by viable cells. While a decrease in overall BPA uptake was observed in the total cell population, the surviving viable cells exhibited relatively increased uptake compared with non-irradiated controls. This apparent discrepancy reflects the fact that IR induced substantial cell death, thereby reducing the absolute uptake at the population level, whereas the residual viable cells responded to radiation-induced stress with enhanced amino acid transporter activity. Several studies have reported a similar phenomenon. Bo *et al* (29) reported that LAT1-mediated amino acid uptake in pancreatic and lung cancer cells was enhanced under conditions of both a high dose rate (such as increased radiation flux or greater dose delivery per unit time) and a high accumulated dose, suggesting that transporter activity is influenced by both the dose rate and the cumulative radiation dose. Additionally, their cells exhibited increased radiosensitivity due to the inhibition of LAT1 expression. The present study demonstrated BPA uptake in TPC-1 cells was predominantly downregulated following exposure to 8 Gy IR, although a relative increase was observed in the surviving viable cell fraction. LAT1 overexpression has been reported to increase BCAA uptake in hepatocellular carcinoma (30,31). While LAT1 functions as a transporter only when complexed with CD98hc on the cell membrane (32), forming a functional heterodimer essential for plasma membrane localization and activity (28), quantitative assessment of this heterodimer via western blotting using whole-cell lysates remains challenging, as membrane-bound and intracellular protein fractions cannot be distinguished, and therefore, do not accurately reflect surface expression (33,34). By contrast, flow cytometry allows for the direct evaluation of membrane-localized LAT1, which is closely associated with CD98hc-mediated transport activity (35,36). Therefore, flow cytometry was used to evaluate functional upregulation of LAT1/CD98hc at the cell surface. Nevertheless, further studies incorporating membrane protein isolation and direct

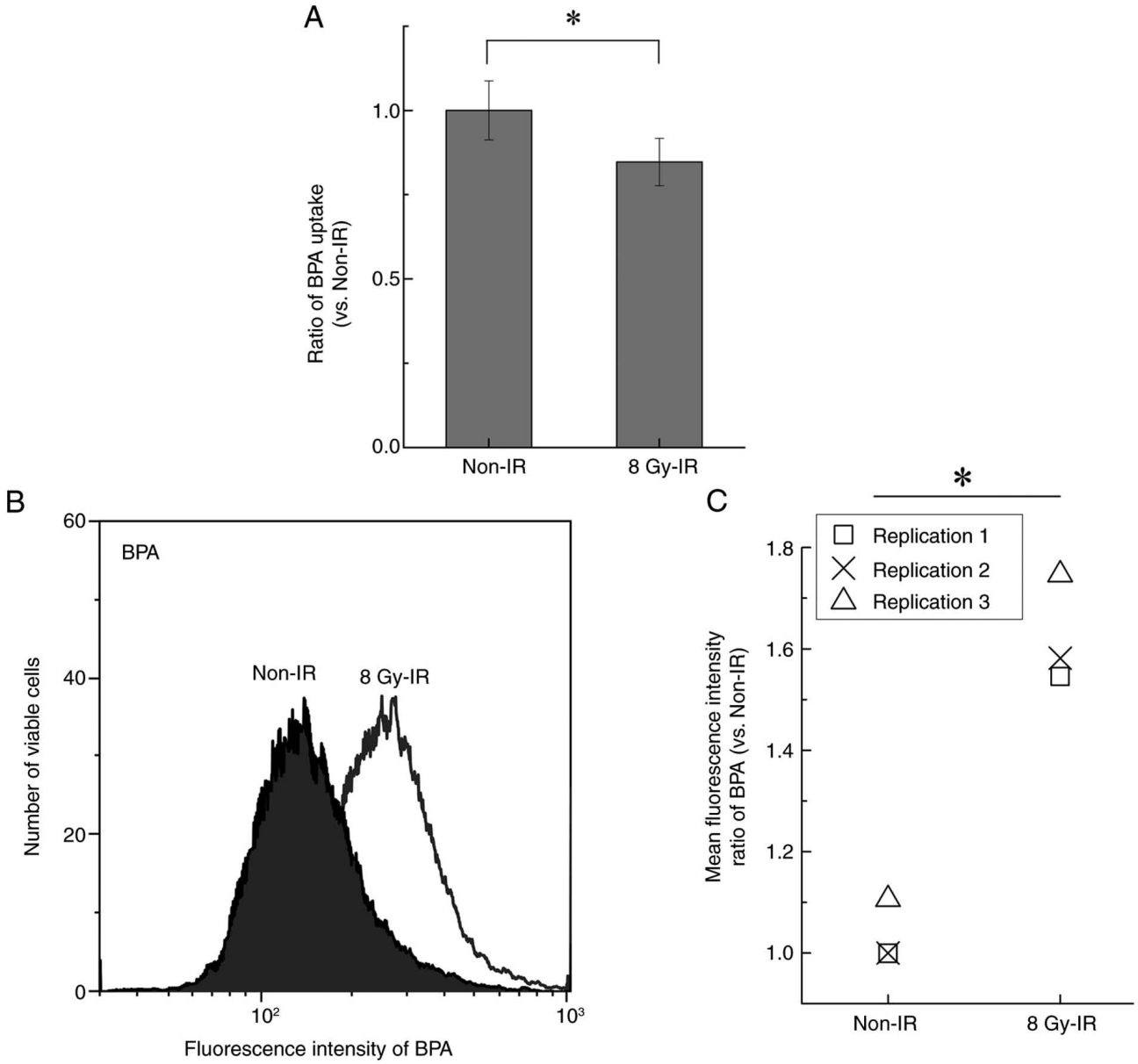

Figure 4. Analysis of BPA uptake. (A) BPA uptake in plated cells exposed to 8 Gy IR was analyzed using a microplate reader. Data are presented as the mean ± SD of the ratio of the IR group (n=6) relative to the control group (n=10). (B) Representative histogram of BPA uptake in single cells analyzed by flow cytometry. (C) Quantification of BPA uptake in single cells (n=3). *P<0.01 (unpaired Student's t-test). BPA, boronophenylalanine; IR, ionizing radiation.

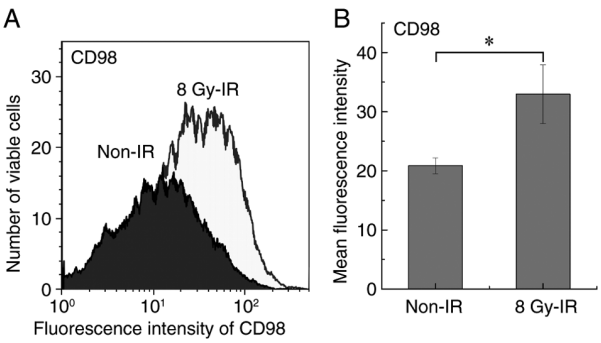

Figure 5. CD98 cell surface antigen expression in TPC-1 cells. (A) Representative flow cytometry histogram. (B) Mean fluorescence intensity of CD98 in cells exposed to IR. Data are presented as the mean ± SD of independent experiments (control, n=3; IR, n=4). *P<0.01 (unpaired Student's t-test). IR, ionizing radiation.

analysis of CD98hc expression are warranted to fully validate the mechanistic role of this transporter system in response to irradiation.

Yoshida *et al* (37) and Matsuya *et al* (38) reported that the BPA uptake in tumor cells was highest in the G_2/M phase compared with other cell cycle phases. These findings and those of the present study indicate that the cellular uptake and serum concentration of BCAAs are involved in LAT1 expression and cell cycle distribution. Conversely, elevated blood BCAA levels have been reported in patients with obesity, insulin resistance and cardiovascular disease (39,40). However, the 3 DTC cases in the present study did not have these conditions. High LAT1 expression has been reported in PTC (41). Based on these findings, the upregulation of serum valine (one of the BCAAs) after ^{131}I treatment with Thyrogen, as shown in the patient analysis in the present study, may

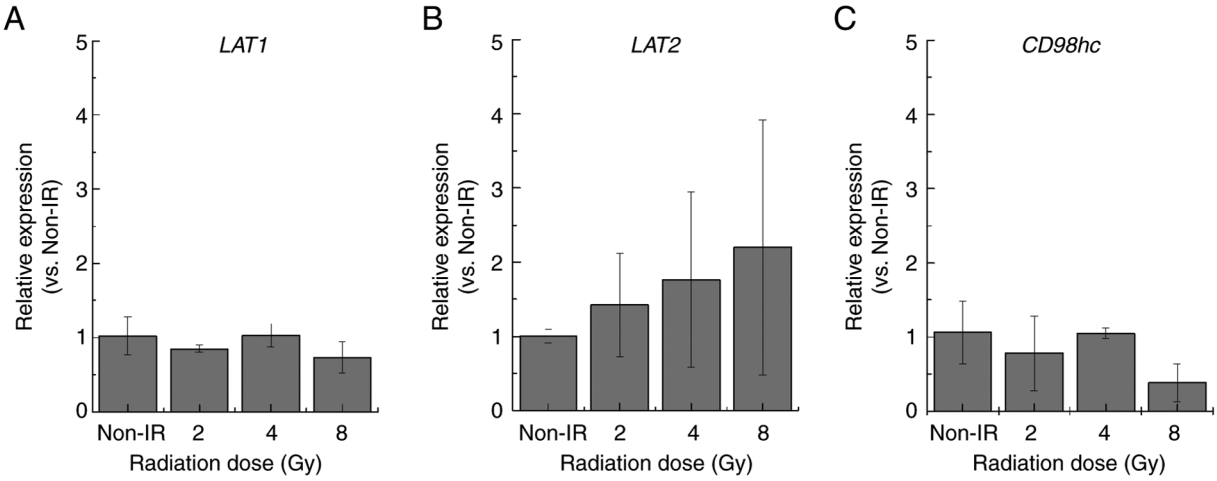

Figure 6. Quantitative mRNA expression analysis via reverse transcription-quantitative PCR. Analysis of (A) *LAT1*, (B) *LAT2* and (C) *CD98hc* mRNA expression in TPC-1 cells after exposure to radiation (2-8 Gy). Data are presented as the mean ± SD of three independent experiments. Statistical analysis was performed using one-way ANOVA followed by the Tukey-Kramer post hoc test; no statistically significant differences were observed among the groups. IR, ionizing radiation; *LAT1*, L-type amino acid transporter type 1; *LAT2*, L-type amino acid transporter type 2.

reflect the fact that valine was not taken up by the tumor. Although leucine and isoleucine also showed an increasing trend, these changes were not statistically significant. These BCAA changes may reflect reduced tumor burden, although direct histopathological confirmation is lacking. In the present *in vitro* experiments, an X-ray dose of 8 Gy was selected based on the clonogenic survival curve of TPC-1 cells, which showed ~1% survival at this dose. This dose was sufficient to elicit measurable biological responses, including changes in amino acid uptake, and is commonly used in mechanistic *in vitro* studies of DNA damage, cell cycle arrest and radiosensitization (21,42,43). Typically, 30-80 Gy are absorbed by the residual thyroid tissue in patients receiving ^{131}I (1.11 GBq) under Thyrogen stimulation depending on remnant size, iodine uptake and kinetics, as calculated using the International Commission on Radiological Protection Publication 106 (44). However, administration of such high doses is not feasible in cell culture due to excessive cytotoxicity (45). Therefore, the use of 8 Gy in the present study represents a biologically relevant and experimentally practical model for evaluating the cellular response to therapeutic radioiodine exposure.

Although ^{131}I is clinically relevant, its uptake relies on the functional NIS, which is minimally expressed in certain thyroid cancer cells, including some differentiated thyroid carcinoma cell lines (3,4). Consequently, ^{131}I-based radiation delivery in such *in vitro* models would be highly variable and non-uniform, reflecting differences in remnant tissue uptake and iodine kinetics observed clinically (5,19,20). By contrast, X-rays provide consistent and uniform exposure in cell culture, making them a practical alternative to assess general radiation-induced stress responses (21,42). While X-rays do not replicate the β-particle emissions or NIS-mediated intracellular effects of ^{131}I, the present approach offers a feasible and relevant model to evaluate LAT1/CD98hc-mediated responses to cytotoxic stress. Future studies using NIS-overexpressing cells or direct ^{131}I labeling will be necessary to clarify ^{131}I-specific mechanisms. However, the biological effects of ^{131}I, primarily through β-particle emissions and active uptake via NIS, are not fully recapitulated by X-ray irradiation (3,5,19,20). The use of TPC-1 cells, which express minimal NIS, limits direct ^{131}I uptake, rendering ^{131}I exposure inconsistent and technically challenging for *in vitro* assays. X-ray irradiation, by contrast, provides a uniform, controllable and reproducible source of IR that induces cytotoxic stress independently of NIS-mediated uptake (21,42). Additionally, the handling of ^{131}I in cell culture requires specialized radiation safety measures, licensing and infrastructure, which could delay exploratory mechanistic studies. Therefore, X-rays were selected as a practical alternative to model general IR-induced stress and to investigate the regulation of amino acid transporter activity, particularly LAT1/CD98hc, under controlled conditions. This is a limitation of the present study, and future studies using NIS-overexpressing cells or direct ^{131}I labeling are needed to elucidate ^{131}I-specific mechanisms.

Exposure of TPC-1 cells to IR induced the expression of the CD98 surface antigen, which may assist in increasing BCAA uptake. BCAAs are essential amino acids mostly supplied through the diet and taken up into tumors by the LAT1-CD98hc complex expressed on the cell membrane (23,27,46). Le Bricon *et al* (47) performed a qualitative analysis using immunohistochemical methods and reported no association between LAT1-positive cancer and BPA uptake. In the present study, the expression levels of the CD98 surface antigen and related mRNAs were quantitatively examined, which is a novel finding. Furthermore, the mRNA expression levels of *LAT1*, *LAT2* and *CD98hc* did not change under exposure to IR based on RT-qPCR. Although *LAT1* and *LAT2* mRNA levels were unchanged, membrane or total protein expression was not assessed due to methodological limitations. Future studies involving membrane protein isolation are needed to clarify whether surface expression of LAT1/LAT2 is altered by irradiation. These findings indicate that the increase in BCAA uptake following IR is a temporary response driven by LAT1 protein already present in the cells, rather than by newly transcribed *LAT1* mRNA. However, further

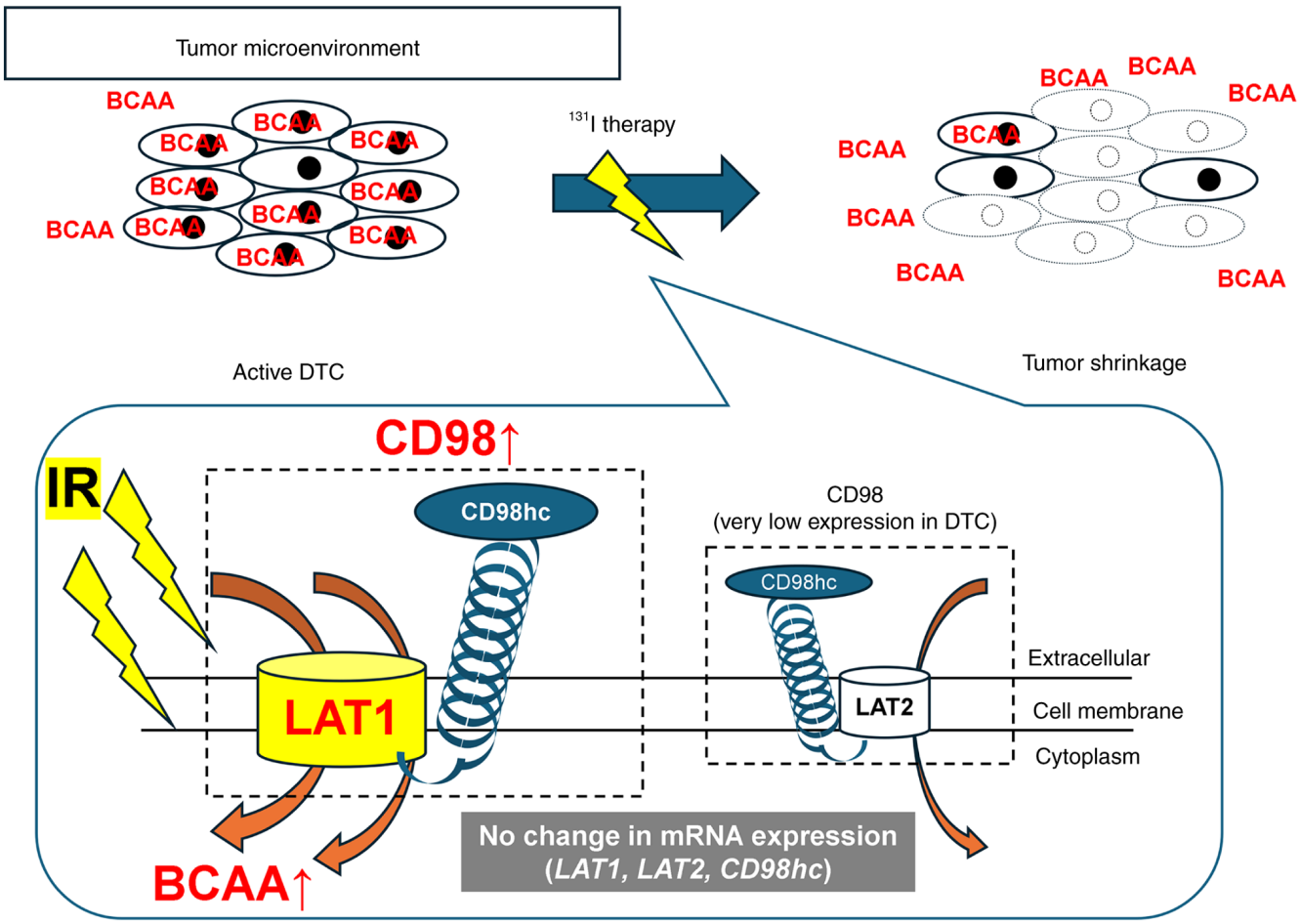

Figure 7. Schematic of the interactions among BCAA, LAT1 and CD98 in the present study. BCAA, branched-chain amino acid; DTC, differentiated thyroid cancer; IR, ionizing radiation; LAT1, L-type amino acid transporter type 1; LAT2, L-type amino acid transporter type 2.

studies are needed to elucidate its molecular mechanism. Furthermore, the interpretation of the increase in serum BCAA levels remains speculative, as histopathological confirmation of the tumor response was not performed in the present study, which analyzed patient samples collected with clinical follow up after obtaining informed consent and ethics approval. The observed changes in BCAA levels may reflect either the release of metabolites from damaged tumor cells or systemic metabolic shifts associated with reduced tumor burden. Although elevated serum BCAA levels may reflect reduced tumor uptake due to LAT1 downregulation, this interpretation should be made with caution, since BCAA levels are also influenced by dietary intake, gastrointestinal absorption, hepatic metabolism and systemic inflammation, including cytokine activity (such as TNF-α), which affects amino acid utilization and appetite (39,40). Furthermore, while LAT1 was upregulated in PTC in previous studies (48,49), its overall contribution to systemic BCAA regulation remains unclear. In the present cases, there was no clinical evidence of recurrence; thus, BCAA changes may reflect systemic metabolic adaptations rather than direct tumor shrinkage. The present *in vitro* data suggested that LAT1/CD98-mediated BCAA uptake represents a mechanism of stress adaptation in surviving cells; however, validation with tissue-level evidence is warranted. This limitation should be addressed in a future prospective cohort study.

Previous studies have demonstrated that *LAT1* expression was upregulated in aggressive variants of DTC and was associated with increased tumor cell proliferation and dedifferentiation, particularly in BRAF-mutant PTC (48,49). This upregulation facilitates increased uptake of essential amino acids, such as BCAAs, supporting tumor metabolism and growth (25,34,35). In this context, the elevated serum BCAA levels observed after ^{131}I treatment may reflect reduced tumor burden and decreased LAT1-mediated amino acid uptake, rather than a mere passive bystander effect. Although the present findings did not establish causality, the consistent increase in serum BCAA concentrations following radioiodine therapy in all patients suggests potential utility as a surrogate biomarker for treatment efficacy. Furthermore, preclinical studies have demonstrated that LAT1 inhibition suppresses tumor growth in thyroid carcinoma (48,49) and hepatocellular carcinoma (30), and has also been implicated in several other cancer types (25,35). Furthermore, LAT1 blockade has been shown to sensitize cancer cells to radiation (29). As summarized in Fig. 7, BCAAs are transported into tumor cells via the LAT1/CD98 complex, IR exposure can transiently increase BCAA uptake in surviving cells, and reduced tumor uptake after ^{131}I therapy may elevate serum BCAA levels. This

integrative mechanism highlights the link between LAT1 activity, amino acid metabolism and treatment response. These observations raise the possibility that LAT1 inhibition could potentiate the therapeutic efficacy of ^{131}I in DTC, especially in tumors with high LAT1 expression (Fig. 7). Further studies are needed to evaluate the translational potential of combining LAT1 inhibitors with radioiodine therapy.

The present study has several limitations. First, the number of patients was small (n=3), which inevitably reduced the statistical power of the clinical findings. Nevertheless, in the absence of prior data on fluctuations in serum BCAA levels in Tg/Ab-positive DTC, this work was designed as a proof-of-concept study. The observed clinical trends were supported by mechanistic experiments using the TPC-1 cell line, which reinforced the biological relevance of BCAA metabolism as a potential surrogate marker of the efficacy of radioiodine therapy. Second, dietary intake of BCAAs was not assessed, which could affect the interpretation of serum metabolite levels. Although all patients fasted for ≥6 h before serum sampling to minimize acute postprandial effects, the influence of habitual dietary intake cannot be completely excluded. To address this, standardized dietary questionnaires or controlled dietary interventions should be incorporated in future studies to clarify the extent to which serum BCAA levels reflect tumor-related metabolic changes rather than nutritional variability. Future studies are also needed to determine whether elevated serum BCAA levels following radioiodine therapy reflect direct release from dying tumor cells, systemic metabolic adaptations due to reduced tumor burden or altered transporter activity in surviving cells. Analysis of associations with tumor histopathology, imaging-based assessments of tumor volume and LAT1/CD98hc expression in clinical specimens will be critical to establish mechanistic links. Additionally, prospective cohort studies with larger sample sizes and standardized dietary assessments are warranted to validate BCAAs as a reliable biomarker for therapeutic efficacy in DTC. Despite unchanged mRNA levels of *LAT1*, *LAT2* and *CD98hc* following IR, flow cytometry demonstrated increased CD98hc surface expression, suggesting post-transcriptional regulation, such as membrane translocation. Notably, the present study assessed mRNA levels at a limited number of time points, which were selected based on feasibility and previous reports (42,43). It is possible that transient fluctuations in gene expression at other time points were missed. Furthermore, radiation-induced gene expression is known to be both dose- and time-dependent (42,43). Further studies are needed to clarify the temporal dynamics of LAT1/CD98hc regulation by evaluating a broader range of radiation doses and time points, and to investigate the mechanistic basis of membrane translocation and its functional consequences in amino acid transport activity.

In patients who are Tg/Ab-positive, monitoring of serum Tg levels can be unreliable due to antibody interference (6-8). The present results suggested that BCAA levels may serve as a complementary biomarker to Tg, providing additional information independent of Tg/Ab status. However, further validation in larger cohorts is necessary to determine whether BCAA monitoring could eventually replace or supplement Tg measurements in clinical practice.

In conclusion, the present findings suggested that an increased extracellular concentration of BCAAs following ^{131}I therapy may reflect a decrease in residual DTC tissue, and thus, may serve as a clinically useful surrogate marker of therapeutic efficacy, particularly in patients for whom traditional Tg-based monitoring is unreliable.

Acknowledgements

The authors would like to thank Mrs. Miyu Miyazaki (Scientific Research Facility Center of Hirosaki University Graduate School of Medicine, Hirosaki, Aomori, Japan) for help with the mass spectrometry, and Mrs. Suzuna Doi (Department of Radiation Science, Hirosaki University Graduate School of Health Sciences, Hirosaki, Aomori, Japan) for her assistance with fluorescence measurements using a microplate reader.

Funding

The present study was supported by JSPS KAKENHI, Grants-in-Aid for Scientific Research (B) (project no. 21H02861/23K21419) and Takeda Science Foundation 2023.

Availability of data and materials

The metabolomics data generated in the present study may be found in the MetaboBank database under accession numbers MTBKS257 and MTBKS258 or at the following URLs: https://ddbj.nig.ac.jp/public/metabobank/study/MTBKS257/ and https://ddbj.nig.ac.jp/public/metabobank/study/MTBKS258/. All other data generated in the present study are included in the figures and/or tables of this article.

Authors' contributions

AK, YM, AW and SM designed the study, drafted the manuscript and actively participated in its revision. AK, YT, RS, YM and SM examined and analyzed the experimental data. YT, YM, AW and SM oversaw the study, and provided final approval of the version submitted and published. YM and SM confirm the authenticity of all the raw data. All authors have read and approved the final version of the manuscript.

Ethics approval and consent to participate

The present study was approved by the Committee of Medical Ethics of the Hirosaki University Graduate School of Health Sciences (approval no. 2021-050; Hirosaki, Japan). Written informed consent was obtained from all participants after providing a detailed verbal explanation, and all collected data were anonymized and handled in accordance with ethical guidelines.

Patient consent for publication

Not applicable.

Competing interests

The authors declare that they have no competing interests.

References

1. Sung H, Ferlay J, Siegel RL, Laversanne M, Soerjomataram I, Jemal A and Bray F: Global cancer statistics 2020: GLOBOCAN estimates of incidence and mortality worldwide for 36 cancers in 185 countries. CA Cancer J Clin 71: 209-249, 2021.
2. Nabhan F, Dedhia PH and Ringel MD: Thyroid cancer, recent advances in diagnosis and therapy. Int J Cancer 149: 984-992, 2021.
3. Haugen BR, Alexander EK, Bible KC, Doherty GM, Mandel SJ, Nikiforov YE, Pacini F, Randolph GW, Sawka AM, Schlumberger M, *et al*: 2015 American thyroid association management guidelines for adult patients with thyroid nodules and differentiated thyroid cancer: The American thyroid association guidelines task force on thyroid nodules and differentiated thyroid cancer. Thyroid 26: 1-133, 2016.
4. Japan Associations of Endocrine Surgery Task Force on the Guidelines for Thyroid Tumors (2024). Clinical practice guidelines on the management of thyroid tumors 2024. Japan Assoc Endocr Surg 41 (Suppl 2): S23-S42, 2024.
5. Hänscheid H, Lassmann M, Luster M, Thomas SR, Pacini F, Ceccarelli C, Ladenson PW, Wahl RL, Schlumberger M, Ricard M, *et al*: Iodine biokinetics and dosimetry in radioiodine therapy of thyroid cancer: Procedures and results of a prospective international controlled study of ablation after rhTSH or hormone withdrawal. J Nucl Med 47: 648-654, 2006.
6. Stanojevic M, Savin S, Cvejic D, Djukic A, Jeremic M and Zivancević Simonovic S: Comparison of the influence of thyroglobulin antibodies on serum thyroglobulin values from two different immunoassays in post surgical differentiated thyroid carcinoma patients. J Clin Lab Anal 23: 341-346, 2009.
7. Spencer CA, Takeuchi M, Kazarosyan M, Wang CC, Guttler RB, Singer PA, Fatemi S, LoPresti JS and Nicoloff JT: Serum thyroglobulin autoantibodies: Prevalence, influence on serum thyroglobulin measurement, and prognostic significance in patients with differentiated thyroid carcinoma. J Clin Endocrinol Metab 83: 1121-1127, 1998.
8. Petrovic I, LoPresti J, Fatemi S, Gianoukakis A, Burman K, Gomez-Lima CJ, Nguyen CT and Spencer CA: Influence of thyroglobulin autoantibodies on thyroglobulin levels measured by different methodologies: IMA, LC-MS/MS, and RIA. J Clin Endocrinol Metab 109: 3254-3263, 2024.
9. Cararo Lopes E, Sawant A, Moore D, Ke H, Shi F, Laddha S, Chen Y, Sharma A, Naumann J, Guo JY, *et al*: Integrated metabolic and genetic analysis reveals distinct features of human differentiated thyroid cancer. Clin Transl Med 13: e1298, 2023.
10. Deja S, Dawiskiba T, Balcerzak W, Orczyk-Pawiłowicz M, Głód M, Pawełka D and Młynarz P: Follicular adenomas exhibit a unique metabolic profile. ^{1}H NMR studies of thyroid lesions. PLoS One 8: e84637, 2013.
11. Abraham T and Schöder H: Thyroid cancer-indications and opportunities for positron emission tomography/computed tomography imaging. Semin Nucl Med 41: 121-138, 2011.
12. Guo L, Zhang Y, Li H, Li S and Guo X: Clinical analysis of influencing factors on therapeutic effect of radioactive iodine therapy in thyroglobulin antibodies positive patients with papillary thyroid cancer. J Nucl Med 63 (Suppl 2): S3006, 2022.
13. Clish CB: Metabolomics: An emerging but powerful tool for precision medicine. Cold Spring Harb Mol Case Stud 1: a000588, 2015.
14. Yu S, Liu C, Hou Y, Li J, Guo Z, Chen X, Zhang L, Peng S, Hong S, Xu L, *et al*: Integrative metabolomic characterization identifies plasma metabolomic signature in the diagnosis of papillary thyroid cancer. Oncogene 41: 2422-2430, 2022.
15. Jiang N, Zhang Z, Chen X, Zhang G, Wang Y, Pan L, Yan C, Yang G, Zhao L, Han J and Xue T: Plasma lipidomics profiling reveals biomarkers for papillary thyroid cancer diagnosis. Front Cell Dev Biol 9: 682269, 2021.
16. Lu J, Hu S, Miccoli P, Zeng Q, Liu S, Ran L and Hu C: Non-invasive diagnosis of papillary thyroid microcarcinoma: A NMR-based metabolomics approach. Oncotarget 7: 81768-81777, 2016.
17. Razavi SA, Mahmanzar M, Nobakht M Gh BF, Zamani Z, Nasiri S and Hedayati M: Plasma metabolites analysis of patients with papillary thyroid cancer: A preliminary untargeted ^{1}H NMR-based metabolomics. J Pharm Biomed Anal 241: 115946, 2024.
18. Monzen S, Tatara Y, Mariya Y, Chiba M, Wojcik A and Lundholm L: HER2-positive breast cancer that resists therapeutic drugs and ionizing radiation releases sphingomyelin-based molecules to circulating blood serum. Mol Clin Oncol 13: 70, 2020.
19. Maxon HR, Thomas SR, Hertzberg VS, Kereiakes JG, Chen IW, Sperling MI and Saenger EL: Relation between effective radiation dose and outcome of radioiodine therapy for thyroid cancer. N Engl J Med 309: 937-941, 1983.
20. Schlesinger T, Flower MA and McCready VR: Radiation dose assessments in radioiodine (131I) therapy. 1. The necessity for in vivo quantitation and dosimetry in the treatment of carcinoma of the thyroid. Radiother Oncol 14: 35-41, 1989.
21. Franken NAP, Rodermond HM, Stap J, Haveman J and van Bree C: Clonogenic assay of cells in vitro. Nat Protoc 1: 2315-2319, 2006.
22. Livak KJ and Schmittgen TD: Analysis of relative gene expression data using real-time quantitative PCR and the 2(-Delta Delta C(T)) method. Methods 25: 402-408, 2001.
23. Untergasser A, Cutcutache I, Koressaar T, Ye J, Faircloth BC, Remm M and Rozen SG: Primer3-new capabilities and interfaces. Nucleic Acids Res 40: e115, 2012.
24. Bustin SA, Benes V, Garson JA, Hellemans J, Huggett J, Kubista M, Mueller R, Nolan T, Pfaffl MW, Shipley GL, *et al*: The MIQE guidelines: Minimum information for publication of quantitative real-time PCR experiments. Clin Chem 55: 611-622, 2009.
25. Kanai Y: Amino acid transporter LAT1 (SLC7A5) as a molecular target for cancer diagnosis and therapeutics. Pharmacol Ther 230: 107964, 2022.
26. Wittig A, Sauerwein WA and Coderre JA: Mechanisms of transport of p-borono-phenylalanine through the cell membrane in vitro. Radiat Res 153: 173-180, 2000.
27. Wongthai P, Hagiwara K, Miyoshi Y, Wiriyasermkul P, Wei L, Ohgaki R, Kato I, Hamase K, Nagamori S and Kanai Y: Boronophenylalanine, a boron delivery agent for boron neutron capture therapy, is transported by ATB0,+, LAT1 and LAT2. Cancer Sci 106: 279-286, 2015.
28. Yan R, Zhao X, Lei J and Zhou Q: Structure of the human LAT1-4F2hc heteromeric amino acid transporter complex. Nature 568: 127-130, 2019.
29. Bo T, Kobayashi S, Inanami O, Fujii J, Nakajima O, Ito T and Yasui H: LAT1 inhibitor JPH203 sensitizes cancer cells to radiation by enhancing radiation-induced cellular senescence. Transl Oncol 14: 101212, 2021.
30. Namikawa M, Kakizaki S, Kaira K, Tojima H, Yamazaki Y, Horiguchi N, Sato K, Oriuchi N, Tominaga H, Sunose Y, *et al*: Expression of amino acid transporters (LAT1, ASCT2 and xCT) as clinical significance in hepatocellular carcinoma. Hepatol Res 45: 1014-1022, 2015.
31. Ericksen RE, Lim SL, McDonnell E, Shuen WH, Vadiveloo M, White PJ, Ding Z, Kwok R, Lee P, Radda GK, *et al*: Loss of BCAA catabolism during carcinogenesis enhances mTORC1 activity and promotes tumor development and progression. Cell Metab 29: 1151-1165.e6, 2019.
32. Kanai Y, Segawa H, Miyamoto K, Uchino H, Takeda E and Endou H: Expression cloning and characterization of a transporter for large neutral amino acids activated by the heavy chain of 4F2 antigen (CD98). J Biol Chem 273: 23629-23632, 1998.
33. Fotiadis D, Kanai Y and Palacín M: The SLC3 and SLC7 families of amino acid transporters. Mol Aspects Med 34: 139-158, 2013.
34. Napolitano L, Scalise M, Galluccio M, Pochini L, Albanese LM and Indiveri C: LAT1 is the transport competent unit of the LAT1/CD98 heterodimeric amino acid transporter. Int J Biochem Cell Biol 67: 25-33, 2015.
35. Häfliger P and Charles RP: The L-type amino acid transporter LAT1-an emerging target in cancer. Int J Mol Sci 20: 2428, 2019.
36. Zhang J, Xu Y, Li D, Fu L, Zhang X, Bao Y and Zheng L: Review of the correlation of LAT1 with diseases: mechanism and treatment. Front Chem 8: 564809, 2020.
37. Yoshida F, Matsumura A, Shibata Y, Yamamoto T, Nakauchi H, Okumura M and Nose T: Cell cycle dependence of boron uptake from two boron compounds used for clinical neutron capture therapy. Cancer Lett 187: 135-141, 2002.
38. Matsuya Y, Sato T, Kusumoto T, Yachi Y, Seino R, Miwa M, Ishikawa M, Matsuyama S and Fukunaga H: Cell-cycle dependence on the biological effects of boron neutron capture therapy and its modification by polyvinyl alcohol. Sci Rep 14: 16696, 2024.
39. Shah SH, Crosslin DR, Haynes CS, Nelson S, Turer CB, Stevens RD, Muehlbauer MJ, Wenner BR, Bain JR, Laferrère B, *et al*: Branched-chain amino acid levels are associated with improvement in insulin resistance with weight loss. Diabetologia 55: 321-330, 2012.

40. McGarrah RW and White PJ: Branched-chain amino acids in cardiovascular disease. Nat Rev Cardiol 20: 77-89, 2023.
41. Wittig A, Sheu-Grabellus SY, Collette L, Moss R, Brualla L and Sauerwein W: BPA uptake does not correlate with LAT1 and Ki67 expressions in tumor samples (results of EORTC trial 11001). Appl Radiat Isot 69: 1807-1812, 2011.
42. Zhao H, Zhuang Y, Li R, Liu Y, Mei Z, He Z, Zhou F and Zhou Y: Effects of different doses of X-ray irradiation on cell apoptosis, cell cycle, DNA damage repair and glycolysis in HeLa cells. Oncol Lett 17: 42-54, 2019.
43. Keam S, MacKinnon KM, D'Alonzo RA, Gill S, Ebert MA, Nowak AK and Cook AM: Effects of photon radiation on DNA damage, cell proliferation, cell survival, and apoptosis of murine and human mesothelioma cell lines. Adv Radiat Oncol 7: 101013, 2022.
44. ICRP: Radiation dose to patients from radiopharmaceuticals. Addendum 3 to ICRP Publication 53. ICRP Publication 106. Approved by the Commission in October 2007. Ann ICRP 38: 1-197, 2008.
45. Du J, Ren W, Liu W, Zhou Y, Li Y, Lai Q, Liu X, Chen T, Liu W, Chen Z, *et al*: Experimental study of iodine-131 labeling of a novel tumor-targeting peptide, TFMP-Y4, in the treatment of hepatocellular carcinoma with internal irradiation. BMC Cancer 25: 245, 2025.
46. Yan R, Li Y, Müller J, Zhang Y, Singer S, Xia L, Zhong X, Gertsch J, Altmann KH and Zhou Q: Mechanism of substrate transport and inhibition of the human LAT1-4F2hc amino acid transporter. Cell Discov 7: 16, 2021.
47. Le Bricon T, Cynober L, Field CJ and Baracos VE: Supplemental nutrition with ornithine alpha-ketoglutarate in rats with cancer-associated cachexia: Surgical treatment of the tumor improves efficacy of nutritional support. J Nutr 125: 2999-3010, 1995.
48. Häfliger P, Graff J, Rubin M, Stooss A, Dettmer MS, Altmann KH, Gertsch J and Charles RP: The LAT1 inhibitor JPH203 reduces growth of thyroid carcinoma in a fully immunocompetent mouse model. J Exp Clin Cancer Res 37: 234, 2018.
49. Enomoto K, Sato F, Tamagawa S, Gunduz M, Onoda N, Uchino S, Muragaki Y and Hotomi M: A novel therapeutic approach for anaplastic thyroid cancer through inhibition of LAT1. Sci Rep 9: 14616, 2019.

Copyright © 2025 Kotani et al. This work is licensed under a Creative Commons Attribution-NonCommercial-NoDerivatives 4.0 International (CC BY-NC-ND 4.0) License.